

Resonance in Cylindrical-Rectangular and Wraparound Microstrip Structures

SAMI M. ALI, SENIOR MEMBER, IEEE, TAREK M. HABASHY, MEMBER, IEEE, JEAN-FU KIANG, AND JIN AU KONG, FELLOW, IEEE

Abstract—A rigorous analysis of the resonance frequency problem of both the cylindrical-rectangular and the wraparound microstrip structure is presented. The problem is formulated in terms of a set of vector integral equations. Using Galerkin's method to solve the integral equations, the complex resonance frequencies are studied with sinusoidal basis functions which incorporate the edge singularity. Furthermore, the complex resonance frequencies are computed using a perturbation approach. Modes suitable for resonator or antenna applications are investigated.

I. INTRODUCTION

CYLINDRICAL microstrip structures are important in many applications where they can be flush-mounted on curved surfaces such as space vehicles, missiles, and boosters [1]. The microstrip antenna elements that are commonly used on these surfaces are of either the wraparound or the cylindrical-rectangular type.

The resonance frequencies of microstrip patches placed on planar structures have been studied extensively [2]–[9]. On the other hand, the resonance frequencies of microstrip patches placed on curved surfaces have attracted less attention. The resonance frequencies of cylindrical-rectangular microstrip patch were calculated using a magnetic wall cavity model [10], thus ignoring the fringing field effects and the radiation loss. In such an analysis, the resonance frequencies obtained are purely real, thus limiting the validity of the obtained results. In [11] the microstrip antennas on cylindrical structures were considered, but no useful results for the resonance problem have been presented.

In this paper, we rigorously analyze the resonance frequency problem of both the cylindrical-rectangular and the wraparound structure using a full-wave approach. The formulation leads to a set of vector integral equations for the current distribution on the conducting patches. This

Manuscript received December 12, 1988; revised July 7, 1989. This work was supported by NASA under Contract NAGW-1272, by RADCOM under Contract F19628-88-K-0013, by the Joint Services Electronics Program under contract DAAL03-89-C-0001, and by the National Science Foundation under Grant 8620029-ECS.

S. M. Ali and J. A. Kong are with the Department of Electrical Engineering and Computer Science, Massachusetts Institute of Technology, Cambridge, MA 02139.

T. M. Habashy is with Schlumberger-Doll Research, Old Quarry Road, Ridgefield, CT 06877-4108.

J.-F. Kiang was with the Department of Electrical Engineering and Computer Science, Massachusetts Institute of Technology, Cambridge, MA. He is now with the IBM Thomas J. Watson Research Center, Yorktown Heights, NY 10598.

IEEE Log Number 8930664.

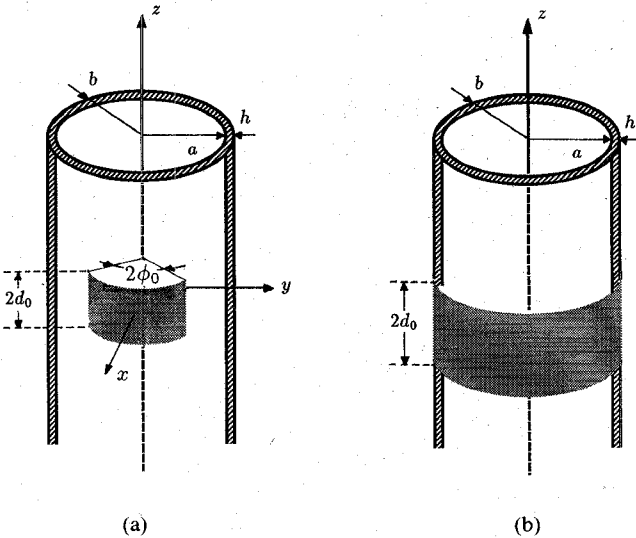


Fig. 1. Geometrical configuration of (a) a cylindrical-rectangular microstrip patch and (b) a wraparound microstrip patch.

set of vector integral equations is then solved using Galerkin's method. Two different sets of basis functions are used to expand the current distribution, one of which takes into account the edge singularity condition. The resulting nonlinear eigenvalue equation is then solved numerically. Both the real and the imaginary part of the complex resonance frequencies are computed as functions of the dielectric substrate thickness. To ascertain the results obtained from the Galerkin method, a perturbation approach based on the single-mode approximation is also used to compute the complex resonance frequencies of the cylindrical-rectangular and wraparound resonators. Different plots for the real and imaginary parts of the resonance frequencies of TE_{01} , HE_{01} , HE_{10} , and HE_{11} are presented.

II. VECTOR INTEGRAL EQUATION FORMULATION

The geometry of the problem is shown in Fig. 1. An infinitely long metallic cylinder of radius a is covered with a dielectric substrate (region 1) of outer radius b , electric permittivity ϵ_1 , and magnetic permeability μ_0 . Region 2 is free space with parameters ϵ_2 and μ_0 . A metallic patch is printed on the surface of the dielectric substrate. The metallic cylinder and the patch are assumed to be perfectly conducting.

For an arbitrary distribution of currents on the metallic patch which vary harmonically as $e^{-i\omega t}$, the z components of the electric and magnetic fields are given by

$$E_z(\rho, \phi, z) = \frac{1}{2\pi} \sum_{n=-\infty}^{\infty} e^{in\phi} \int_{-\infty}^{\infty} dk_z e^{ik_z z} \cdot \begin{cases} A_1^{(e)} H_n^{(1)}(k_{1\rho}\rho) + B_1^{(e)} J_n(k_{1\rho}\rho), & a < \rho < b \\ A_2^{(e)} H_n^{(1)}(k_{2\rho}\rho), & b < \rho \end{cases} \quad (1a)$$

$$H_z(\rho, \phi, z) = \frac{1}{2\pi} \sum_{n=-\infty}^{\infty} e^{in\phi} \int_{-\infty}^{\infty} dk_z e^{ik_z z} \cdot \begin{cases} A_1^{(h)} H_n^{(1)}(k_{1\rho}\rho) + B_1^{(h)} J_n(k_{1\rho}\rho), & a < \rho < b \\ A_2^{(h)} H_n^{(1)}(k_{2\rho}\rho), & b < \rho \end{cases} \quad (1b)$$

where the field spectral amplitudes $A_1^{(e)}$, $A_2^{(e)}$, $B_1^{(e)}$, $A_1^{(h)}$, $A_2^{(h)}$, and $B_1^{(h)}$ are functions of the harmonic order n and the spectral variable k_z and

$$k_1^2 - k_{1\rho}^2 = k_z^2 = k_2^2 - k_{2\rho}^2.$$

By imposing the boundary conditions on the tangential components of the electric field (E_z and E_ϕ) at the perfectly conducting inner cylinder ($\rho = a$), we obtain the following relationships between the spectral amplitudes:

$$B_1^{(e)} = -\eta_i A_1^{(e)} \quad (2a)$$

$$B_1^{(h)} = -\xi_i A_1^{(h)} \quad (2b)$$

where

$$\eta_i = \frac{H_n^{(1)}(k_{1\rho}a)}{J_n(k_{1\rho}a)} \quad (3a)$$

$$\xi_i = \frac{H_n^{(1)'}(k_{1\rho}a)}{J_n'(k_{1\rho}a)}. \quad (3b)$$

By matching the tangential components of the electric field (E_z and E_ϕ) across the boundary at $\rho = b$, we get

$$A_1^{(e)} = \frac{H_n^{(1)}(k_{2\rho}b)}{J_n(k_{1\rho}b)} \frac{1}{\eta_0 - \eta_i} A_2^{(e)} \quad (4a)$$

$$A_1^{(h)} = \frac{H_n^{(1)}(k_{2\rho}b)}{J_n(k_{1\rho}b)} \frac{1}{\xi_0 - \xi_i} \left[\frac{k_{1\rho}}{k_{2\rho}} \frac{\alpha}{\beta} A_2^{(h)} - (\epsilon_r - 1) \frac{i\omega\epsilon_2}{k_{2\rho}} \frac{k_z}{k_{2\rho}} \frac{n}{k_{1\rho}b} \frac{1}{\beta} A_2^{(e)} \right] \quad (4b)$$

where

$$\eta_0 = \frac{H_n^{(1)}(k_{1\rho}b)}{J_n(k_{1\rho}b)} \quad (5a)$$

$$\xi_0 = \frac{H_n^{(1)'}(k_{1\rho}b)}{J_n'(k_{1\rho}b)} \quad (5b)$$

$$\beta = \frac{J_n'(k_{1\rho}b)}{J_n(k_{1\rho}b)} \quad (5c)$$

$$\alpha = \frac{H_n^{(1)'}(k_{2\rho}b)}{H_n^{(1)}(k_{2\rho}b)} \quad (5d)$$

and

$$\epsilon_r = \frac{\epsilon_1}{\epsilon_2}.$$

We notice from (4) that cross-polarization occurs. With the exception of the $n = 0$ case, the normal modes are no longer pure TE or TM. These hybrid modes are commonly classified as HE_{nm} or EH_{nm} , which, respectively, tend to TE_{nm} and TM_{nm} for vanishingly thin substrate.

Next we will derive an expression which relates the current on the patch to the spectral amplitudes of the fields. To do so, we match the discontinuity in the tangential components of the magnetic field (H_z and H_ϕ) to the current on the patch. Then, applying the orthogonality relationships on the Fourier series expansion with respect to ϕ and the Fourier transform with respect to z , and using (2) and (4), we obtain a relationship between the surface current and the field spectral amplitudes as follows:

$$\mathbf{J}_n(k_z) = \bar{\bar{X}}_n(k_z) \cdot \mathbf{a}_2 \quad (6)$$

where

$$\mathbf{J}_n(k_z) = \begin{bmatrix} J_{\phi n}(k_z) \\ J_{zn}(k_z) \end{bmatrix} = \frac{1}{2\pi} \int_{-\pi}^{\pi} d\phi e^{-in\phi} \int_{-\infty}^{\infty} dz e^{-ik_z z} \mathbf{J}(\phi, z) \quad (7)$$

$$\mathbf{a}_2 = \begin{bmatrix} A_2^{(e)} \\ A_2^{(h)} \end{bmatrix} H_n^{(1)}(k_{2\rho}b) \quad (8)$$

$$\bar{\bar{X}}_n(k_z) = \begin{bmatrix} X_{11} & X_{12} \\ X_{21} & X_{22} \end{bmatrix} \quad (9)$$

and

$$X_{11} = -(\epsilon_r - 1) \frac{i\omega\epsilon_2}{k_{2\rho}} \frac{k_z}{k_{2\rho}} \frac{n}{k_{1\rho}b} \frac{1}{\beta} r^{(h)} \quad (10a)$$

$$X_{12} = -\left[1 - \frac{k_{1\rho}}{k_{2\rho}} \frac{\alpha}{\beta} r^{(h)} \right] \quad (10b)$$

$$X_{21} = \frac{i\omega\epsilon_2}{k_{2\rho}} \left[\alpha - \epsilon_r \beta \frac{k_{2\rho}}{k_{1\rho}} r^{(e)} - (\epsilon_r - 1) \frac{k_{2\rho}}{k_{1\rho}} \left(\frac{k_z}{k_{2\rho}} \right)^2 \left(\frac{n}{k_{1\rho}b} \right)^2 \frac{1}{\beta} r^{(h)} \right] \quad (10c)$$

$$X_{22} = -\frac{k_z}{k_{2\rho}} \frac{n}{k_{2\rho}b} \left[1 - \frac{k_{2\rho}}{k_{1\rho}} \frac{\alpha}{\beta} r^{(h)} \right] \quad (10d)$$

$$r^{(h)} = \frac{\eta_0 - \xi_i}{\xi_0 - \xi_i} \quad (11a)$$

$$r^{(e)} = \frac{\xi_0 - \eta_i}{\eta_0 - \eta_i} \quad (11b)$$

On the other hand, the Fourier transforms of the tangential components of the electric field at $\rho = b$ are related to the field spectral amplitudes as follows:

$$\mathbf{E}_{sn}(k_z) = \bar{\bar{S}}_n(k_z) \cdot \mathbf{a}_2 \quad (12)$$

where

$$\begin{aligned} \mathbf{E}_{sn}(k_z) &= \begin{bmatrix} E_{\phi n}(k_z) \\ E_{z n}(k_z) \end{bmatrix} \\ &= \frac{1}{2\pi} \int_{-\pi}^{\pi} d\phi e^{-in\phi} \int_{-\infty}^{\infty} dz e^{-ik_z z} \mathbf{E}_s(\phi, z) \quad (13) \end{aligned}$$

$$\bar{\bar{S}}_n(k_z) = \begin{bmatrix} S_{11} & S_{12} \\ S_{21} & S_{22} \end{bmatrix} \quad (14)$$

$$S_{11} = -\frac{k_z}{k_{2\rho}} \frac{n}{k_{2\rho} b} \quad (15a)$$

$$S_{12} = -\frac{i\omega\epsilon_0}{k_{2\rho}} \alpha \quad (15b)$$

$$S_{21} = 1 \quad (15c)$$

$$S_{22} = 0. \quad (15d)$$

Thus from (6) and (12), we obtain the following relationship between the patch current and the electric field on the patch represented in the spectral domain:

$$\mathbf{E}_{sn}(k_z) = \bar{\bar{\Gamma}}_n(k_z) \cdot \mathbf{J}_n(k_z) \quad (16)$$

where $\bar{\bar{\Gamma}}_n(k_z)$ can be obtained from (10) and (15) as follows:

$$\bar{\bar{\Gamma}}_n(k_z) = \begin{bmatrix} \Gamma_{11} & \Gamma_{12} \\ \Gamma_{21} & \Gamma_{22} \end{bmatrix} \quad (17)$$

$$\begin{aligned} \Gamma_{11} &= \frac{1}{\Delta} \left[\left(\frac{k_z}{k_{2\rho}} \right)^2 \left(\frac{n}{k_{2\rho} b} \right)^2 \left\{ 1 - \frac{\alpha}{\beta} \left(\frac{k_{2\rho}}{k_{1\rho}} \right)^3 r^{(h)} \right\} \right. \\ &\quad \left. - \left(\frac{k_z}{k_{2\rho}} \right)^2 \alpha \left\{ \alpha - \epsilon_r \beta \frac{k_{2\rho}}{k_{1\rho}} r^{(e)} \right\} \right] \quad (18a) \end{aligned}$$

$$\Gamma_{12} = \Gamma_{21} = -\frac{1}{\Delta} \frac{k_z}{k_{2\rho}} \frac{n}{k_{2\rho} b} \left[1 - \frac{k_{2\rho}}{k_{1\rho}} \frac{\alpha}{\beta} r^{(h)} \right] \quad (18b)$$

$$\Gamma_{22} = \frac{1}{\Delta} \left[1 - \frac{k_{1\rho}}{k_{2\rho}} \frac{\alpha}{\beta} r^{(h)} \right] \quad (18c)$$

and Δ is the determinant of $\bar{\bar{\Gamma}}_n(k_z)$, given by

$$\begin{aligned} \Delta &= \frac{i\omega\epsilon_2}{k_{2\rho}} \left[\left\{ \alpha - \epsilon_r \beta \frac{k_{2\rho}}{k_{1\rho}} r^{(e)} \right\} \left\{ 1 - \frac{k_{1\rho}}{k_{2\rho}} \frac{\alpha}{\beta} r^{(h)} \right\} \right. \\ &\quad \left. + (\epsilon_r - 1)^2 \frac{k_z^2}{k_{1\rho} k_{2\rho}} \left(\frac{k_z}{k_{2\rho}} \right)^2 \left(\frac{n}{k_{1\rho} b} \right)^2 \frac{1}{\beta} r^{(h)} \right]. \quad (19) \end{aligned}$$

Note that the matrix $\bar{\bar{\Gamma}}_n(k_z)$ is symmetric ($\Gamma_{21} = \Gamma_{12}$), which is a consequence of reciprocity. Using (4) and (6),

the field spectral amplitudes in region 1 can be obtained as

$$\mathbf{a}_1 = \bar{\bar{Y}}_n(k_z) \cdot \mathbf{J}_n(k_z) \quad (20)$$

where

$$\mathbf{a}_1 = \begin{bmatrix} A_1^{(e)} \\ A_1^{(h)} \end{bmatrix} J_n(k_{1\rho} b) \quad (21)$$

$$\bar{\bar{Y}}_n(k_z) = \begin{bmatrix} Y_{11} & Y_{12} \\ Y_{21} & Y_{22} \end{bmatrix} \quad (22)$$

$$Y_{11} = -\frac{1}{\Delta} \frac{k_z}{k_{2\rho}} \frac{n}{k_{2\rho} b} \left[1 - \frac{k_{2\rho}}{k_{1\rho}} \frac{\alpha}{\beta} r^{(h)} \right] \frac{1}{\eta_0 - \eta_i} \quad (23a)$$

$$Y_{12} = \frac{1}{\Delta} \left[1 - \frac{k_{1\rho}}{k_{2\rho}} \frac{\alpha}{\beta} r^{(h)} \right] \frac{1}{\eta_0 - \eta_i} \quad (23b)$$

$$\begin{aligned} Y_{21} &= \frac{1}{\Delta} \frac{i\omega\epsilon_2}{k_{2\rho}} \frac{k_{1\rho}}{k_{2\rho}} \frac{1}{\beta} \left[(\epsilon_r - 1) \left(\frac{k_z}{k_{2\rho}} \right)^2 \left(\frac{n}{k_{1\rho} b} \right)^2 \right. \\ &\quad \left. - \alpha \left\{ \alpha - \epsilon_r \beta \frac{k_{2\rho}}{k_{1\rho}} r^{(e)} \right\} \right] \frac{1}{\xi_0 - \xi_i} \quad (23c) \end{aligned}$$

$$Y_{22} = -(\epsilon_r - 1) \frac{1}{\Delta} \frac{i\omega\epsilon_2}{k_{2\rho}} \frac{k_z}{k_{2\rho}} \frac{n}{k_{2\rho} b} \frac{1}{\beta} \frac{1}{\xi_0 - \xi_i} \quad (23d)$$

where Δ is given by (19).

Imposing the mixed boundary conditions at $\rho = b$ on the tangential components of the electric field $\mathbf{E}_s(\phi, z)$ and on the current density $\mathbf{J}(\phi, z)$, we obtain a set of vector integral equations given by

$$\mathbf{E}_s(\phi, z) = \frac{1}{2} \sum_{n=-\infty}^{\infty} e^{in\phi} \int_{-\infty}^{\infty} dk_z e^{ik_z z} \bar{\bar{\Gamma}}_n(k_z) \cdot \mathbf{J}_n(k_z) = 0 \quad \text{on the patch} \quad (24)$$

$$\mathbf{J}(\phi, z) = \frac{1}{2\pi} \sum_{n=-\infty}^{\infty} e^{in\phi} \int_{-\infty}^{\infty} dk_z e^{ik_z z} \mathbf{J}_n(k_z) = 0 \quad \text{outside the patch.} \quad (25)$$

The next step is to solve this set of vector integral equations using the Galerkin method.

III. GALERKIN'S METHOD

Now we solve the set of dual integral equations (24) and (25) by using Galerkin's method. We expand the current $\mathbf{J}(\phi, z)$ in terms of a set of basis functions which is complete over the support of the patch:

$$\begin{aligned} \mathbf{J}(\phi, z) &= \sum_{n,m} \bar{\bar{K}}_{nm}(\phi, z) \cdot \mathbf{A}_{nm} \quad \text{on the patch} \\ &= 0 \quad \text{outside the patch.} \quad (26) \end{aligned}$$

The spectral components of this current distribution are given by

$$\begin{aligned} \mathbf{J}_r(k_z) &= \frac{1}{2\pi} \int_{-\pi}^{\pi} d\phi e^{-in\phi} \int_{-d_0}^{d_0} dz e^{-ik_z z} \mathbf{J}(\phi, z) \\ &= \sum_{n,m} \bar{\bar{T}}_{r,nm}(k_z) \cdot \mathbf{A}_{nm} \quad (27) \end{aligned}$$

where

$$\bar{\bar{T}}_{r,nm}(k_z) = \frac{1}{2\pi} \int_{-\pi}^{\pi} d\phi e^{-ir\phi} \int_{-d_0}^{d_0} dz e^{-ik_z z} \bar{\bar{K}}_{nm}(\phi, z). \quad (28)$$

Substituting (27) into (24), we obtain

$$\sum_{r=-\infty}^{\infty} e^{ir\phi} \int_{-\infty}^{\infty} dk_z e^{ik_z z} \bar{\bar{T}}_r(k_z) \cdot \sum_{n,m} \bar{\bar{T}}_{r,nm}(k_z) \cdot \mathbf{A}_{nm} = 0$$

on the patch. (29)

Next, the above equation is tested by the same set of basis functions that was used in the expansion of the patch current. This is done by premultiplying (29) by $\bar{\bar{K}}_{pq}^{\dagger}(\phi, z)$ and integrating over the patch area. Thus we get

$$\sum_{n,m} \bar{\bar{Q}}_{pq,nm} \cdot \mathbf{A}_{nm} = 0 \quad (30)$$

where

$$\bar{\bar{Q}}_{pq,nm} = \int_{-\infty}^{\infty} dk_z \sum_{r=-\infty}^{\infty} \bar{\bar{T}}_{r,pq}^{\dagger}(k_z^*) \cdot \bar{\bar{T}}_r(k_z) \cdot \bar{\bar{T}}_{r,nm}(k_z).$$

(31)

Nontrivial solutions can exist if the determinant of (30) vanishes, that is,

$$\det |\bar{\bar{Q}}_{pq,nm}| = f(\omega) = 0. \quad (32)$$

This is the eigenvalue equation for the cylindrical microstrip resonator. The roots of this equation are complex numbers, indicating that the structure has complex resonance frequencies. The imaginary part of the complex resonance frequencies accounts for the radiation loss.

Now, we apply the above formulation to find the resonance frequencies of the cylindrical-rectangular microstrip patch shown in Fig. 1(a) and the wraparound patch of Fig. 1(b).

In choosing the set of basis functions for the expansion of the patch current, one has to ensure that the normal component of the current vanishes at the edge whereas the tangential component satisfies the edge condition. Thus, for the wraparound patch,

$$\bar{\bar{K}}_{nm}(\phi, z) = e^{in\phi} \bar{\bar{\Omega}}_m(z) \quad (33)$$

where $-\pi \leq \phi \leq \pi$, and

$$\bar{\bar{\Omega}}_m(z) = \begin{bmatrix} \frac{1}{\sqrt{d_0^2 - z^2}} \cos \left\{ \frac{m\pi}{2d_0} (z + d_0) \right\} & 0 \\ 0 & \sin \left\{ \frac{m\pi}{2d_0} (z + d_0) \right\} \end{bmatrix}. \quad (34)$$

In this case we have

$$\bar{\bar{T}}_{r,nm}(k_z) = \delta_{nr} i^m \begin{bmatrix} \frac{\pi}{2} \left\{ J_0 \left(\frac{m\pi}{2} - k_z d_0 \right) + (-1)^m J_0 \left(\frac{m\pi}{2} + k_z d_0 \right) \right\} & 0 \\ 0 & i 2 \left(\frac{m\pi}{2d_0} \right) \frac{\sin \left(\frac{m\pi}{2} - k_z d_0 \right)}{k_z^2 - \left(\frac{m\pi}{2d_0} \right)^2} \end{bmatrix}. \quad (35)$$

For the cylindrical-rectangular patch,

$$\bar{\bar{K}}_{nm}(\phi, z) = \bar{\bar{\Theta}}_n(\phi) \cdot \bar{\bar{\Omega}}_m(z) \quad (36)$$

where $-\phi_0 \leq \phi \leq \phi_0$ and zero otherwise, and

$$\bar{\bar{\Theta}}_n(\phi) = \begin{bmatrix} \sin \left\{ \frac{n\pi}{2\phi_0} (\phi + \phi_0) \right\} & 0 \\ 0 & \frac{1}{\sqrt{\phi_0^2 - \phi^2}} \cos \left\{ \frac{n\pi}{2\phi_0} (\phi + \phi_0) \right\} \end{bmatrix}. \quad (37)$$

In this case we have

$$\bar{\bar{T}}_{r,nm}(k_z) = \frac{1}{2} i^{n+m+1} \begin{bmatrix} \left(\frac{n\pi}{2\phi_0}\right) \frac{\sin\left(\frac{n\pi}{2} - r\phi_0\right)}{r^2 - \left(\frac{n\pi}{2\phi_0}\right)^2} & 0 \\ 0 & \left\{ J_0\left(\frac{n\pi}{2} - r\phi_0\right) + (-1)^n J_0\left(\frac{n\pi}{2} + r\phi_0\right) \right\} \\ \left\{ J_0\left(\frac{m\pi}{2} - k_z d_0\right) + (-1)^m J_0\left(\frac{m\pi}{2} + k_z d_0\right) \right\} & 0 \\ 0 & \left(\frac{m\pi}{2d_0}\right) \frac{\sin\left(\frac{m\pi}{2} - k_z d_0\right)}{k_z^2 - \left(\frac{m\pi}{2d_0}\right)^2} \end{bmatrix}. \quad (38)$$

Using the explicit expressions of $\bar{\bar{\Gamma}}_n(k_z)$ given by (18) together with (35), equation (31) reduces to

$$\bar{\bar{Q}}_{pq,nm} = \delta_{pn} 2 \left[1 + (-1)^{q+m} \right] \int_0^\infty dk_z \bar{\bar{T}}_{n,nq}^\dagger(k_z^*) \cdot \bar{\bar{\Gamma}}_n(k_z) \cdot \bar{\bar{T}}_{r,nm}(k_z) \quad (39)$$

for the wraparound patch.

Similarly, from (18) together with (38), equation (31) reduces to

$$\bar{\bar{Q}}_{pq,nm} = \left[1 + (-1)^{p+n} \right] \left[1 + (-1)^{q+m} \right] \int_0^\infty dk_z \sum_{r=0}^\infty \frac{1}{1 + \delta_{r0}} \bar{\bar{T}}_{r,pq}^\dagger(k_z^*) \cdot \bar{\bar{T}}_{r,nm}(k_z) \quad (40)$$

for the cylindrical-rectangular patch.

IV. PERTURBATION FORMULA FOR THE RESONANCE FREQUENCIES

In the limit of a thin substrate, the resonance frequencies approach that of the magnetic-wall cavity, and a perturbation approach can be used to calculate the resonance frequencies. In this limit, the cylindrical microstrip structure can be viewed as a perturbation of a cylindrical resonator with perfectly magnetic sidewalls. The resonance frequency shift of this perturbed magnetic wall cavity resonator can be computed as [4], [12]

$$\Delta\omega = \omega_f - \omega_i \approx \frac{L}{4\langle W_T \rangle_i} \quad (41)$$

where

$$L = -i \int \int_{\Delta S} dS \hat{n} \cdot (E_i^* \times H_f) \quad (42)$$

and

$$\langle W_T \rangle_i = \frac{1}{2} \epsilon_1 \iiint_V dV |E_i|^2 \quad (43)$$

where E_i and ω_i are the electric field and the resonance frequency of the unperturbed cavity; H_f and ω_f are the

magnetic field and the resonance frequency of the perturbed cavity (i.e., the open cavity); $\langle W_T \rangle_i$ is the unperturbed time-averaged total energy stored in the cavity; and ΔS is the surface area of the sidewalls. In the unperturbed case, the field components are independent of ρ since the substrate thickness is assumed thin. Thus, the only existing modes are the TE_{nm} modes, for which E_ρ is the only nonvanishing electric field component. Thus (42) can be written as

$$L = -i \int \int_{\Delta S} dS E_{\rho i}^* \left[-\hat{\phi} H_{zf} + \hat{z} H_{\phi f} \right] \cdot \hat{n} \quad (44)$$

where H_{zf} and $H_{\phi f}$ can be expressed in terms of the patch's current spectral amplitude as

$$H_{zf}(\rho, \phi, z) = \frac{1}{2\pi} \sum_{r=-\infty}^{\infty} e^{ir\phi} \int_{-\infty}^{\infty} dk_z e^{ik_z z} \mathbf{R}_{zr}^t(\rho, k_z) \cdot \bar{\bar{Y}}_r(k_z) \cdot \mathbf{J}_r(k_z) \quad (45a)$$

$$H_{\phi f}(\rho, \phi, z) = \frac{1}{2\pi} \sum_{r=-\infty}^{\infty} e^{ir\phi} \int_{-\infty}^{\infty} dk_z e^{ik_z z} \mathbf{R}_{\phi r}^t(\rho, k_z) \cdot \bar{\bar{F}}(k_z) \cdot \bar{\bar{Y}}_r(k_z) \cdot \mathbf{J}_r(k_z) \quad (45b)$$

where

$$\mathbf{R}_{zr}(\rho, k_z) = \begin{bmatrix} 0 \\ 1 \end{bmatrix} \frac{H_r^{(1)}(k_{1\rho}\rho) - \xi_r J_r(k_{1\rho}\rho)}{J_r(k_{1\rho}b)} \quad (46)$$

$$\mathbf{R}_{\phi r}(\rho, k_z) = \frac{1}{J_r(k_{1\rho}b)} \begin{bmatrix} H_r^{(1)\prime}(k_{1\rho}\rho) - \eta_r J_r'(k_{1\rho}\rho) \\ \frac{r}{k_{1\rho}\rho} [H_r^{(1)}(k_{1\rho}\rho) - \xi_r J_r(k_{1\rho}\rho)] \end{bmatrix} \quad (47)$$

$$\bar{\bar{F}}(k_z) = \begin{bmatrix} \frac{i\omega\epsilon_1}{k_{1\rho}} & 0 \\ 0 & -\frac{k_z}{k_{1\rho}} \end{bmatrix} \quad (48)$$

and $\bar{\bar{Y}}_r(k_z)$ is given by (22).

Let us consider the perturbation of a TE_{nm} mode whose unperturbed resonance frequency is ω_{nm} given by

$$\omega_{nm} = \frac{k_{nm}}{\sqrt{\mu_0\epsilon_1}} = \frac{1}{\sqrt{\mu_0\epsilon_1}} \sqrt{\left(\frac{n}{a}\right)^2 + \left(\frac{m\pi}{2d_0}\right)^2} \quad (49)$$

for the wraparound patch, and

$$\omega_{nm} = \frac{k_{nm}}{\sqrt{\mu_0\epsilon_1}} = \frac{1}{\sqrt{\mu_0\epsilon_1}} \sqrt{\left(\frac{n\pi}{2\phi_0 a}\right)^2 + \left(\frac{m\pi}{2d_0}\right)^2} \quad (50)$$

for the cylindrical-rectangular patch.

The difference between (49) and (50) when $\phi_0 = \pi$ is due to the different boundary conditions satisfied by the current at the edge of the patches. The current J_ϕ has to vanish at $\phi = \phi_0$ for the rectangular cylindrical patch, which is not the case for the wraparound patch.

For this mode of the wraparound patch, the unperturbed electric field is given by

$$E_{\rho i}(\phi, z) = E_{nm} e^{in\phi} \cos\left[\frac{m\pi}{2d_0}(z + d_0)\right] \quad (51)$$

and the patch current is given by

$$J_i(\phi, z) = \frac{1}{i\omega_{nm}\mu_0} E_{nm} e^{in\phi} \bar{\Omega}_m(z) \cdot \tau_{nm} \quad (52a)$$

where

$$\tau_{nm} = \begin{bmatrix} -\frac{in}{b} \\ \frac{m\pi}{2d_0} \end{bmatrix} \approx \begin{bmatrix} -\frac{in}{a} \\ \frac{m\pi}{2d_0} \end{bmatrix}. \quad (52b)$$

The unperturbed time-averaged total energy stored in the wraparound cavity can be obtained as

$$\langle W_T \rangle_i \approx \pi a \epsilon_1 |E_{nm}|^2 (1 + \delta_{m0}) h d_0 \quad (53)$$

where $h = b - a$.

For the cylindrical-rectangular patch, the unperturbed electric field is given by

$$E_{\rho i}(\phi, z) = E_{nm} \cos\left[\frac{n\pi}{2\phi_0}(\phi + \phi_0)\right] \cos\left[\frac{m\pi}{2d_0}(z + d_0)\right] \quad (54)$$

and the patch current has the form

$$J_i(\phi, z) = \frac{1}{i\omega_{nm}\mu_0} E_{nm} \bar{\Theta}_n(\phi) \cdot \bar{\Omega}_m(z) \cdot \tau_{nm} \quad (55a)$$

where

$$\tau_{nm} = \begin{bmatrix} \frac{n\pi}{2\phi_0 b} \\ \frac{m\pi}{2d_0} \end{bmatrix} \approx \begin{bmatrix} \frac{n\pi}{2\phi_0 a} \\ \frac{m\pi}{2d_0} \end{bmatrix}. \quad (55b)$$

The unperturbed time-averaged total energy stored in the cylindrical-rectangular cavity can be represented by the following expression:

$$\langle W_T \rangle_i \approx \frac{1}{2} \epsilon_1 |E_{nm}|^2 (1 + \delta_{m0}) (1 + \delta_{m0}) \phi_0 a h d_0. \quad (56)$$

In both the wraparound and the cylindrical-rectangular case, the Fourier transform of the patch's current in the unperturbed state is given by

$$\mathbf{J}_r^{(i)}(k_z) = \frac{1}{i\omega_{nm}\mu_0} E_{nm} \bar{\bar{T}}_{r,nm}(k_z) \cdot \tau_{nm}. \quad (57)$$

In the limit when $h/a \rightarrow 0$, the patch current can be approximated by its value in the unperturbed state and hence

$$\mathbf{J}_r(k_z) \approx \mathbf{J}_r^{(i)}(k_z). \quad (58)$$

Thus, in the thin substrate limit, using (51), approximate expressions for the magnetic field components H_{zf} and $H_{\phi f}$ can be obtained.

For the wraparound patch, using (44) we can get

$$L \approx \frac{2i a h}{\pi \omega_{nm} \mu_0} |E_{nm}|^2 \left[-(-1)^m \int_{-\infty}^{\infty} dk_z e^{ik_z d_0} \mathbf{R}_{\phi n}^t(k_z) \cdot \bar{\bar{F}}(k_z) \cdot \bar{\bar{Y}}_n(k_z) \cdot \bar{\bar{T}}_{n,nm}(k_z) \right. \\ \left. + \int_{-\infty}^{\infty} dk_z e^{-ik_z d_0} \mathbf{R}_{\phi n}^t(k_z) \cdot \bar{\bar{F}}(k_z) \cdot \bar{\bar{Y}}_n(k_z) \cdot \bar{\bar{T}}_{n,nm}(k_z) \right] \cdot \tau_{nm} \quad (59)$$

where

$$\mathbf{R}_{\phi n}(k_z) = \frac{\pi}{2i a h} \int_a^b d\rho \rho \mathbf{R}_{\phi n}(\rho, k_z) \\ \approx \frac{1}{k_{1\rho} a} \frac{1}{J_n(k_{1\rho} a)} \begin{bmatrix} \frac{1}{J_n(k_{1\rho} a)} \\ -\frac{n}{k_{1\rho} a} \frac{1}{J_n'(k_{1\rho} a)} \end{bmatrix}. \quad (60)$$

It can be easily shown that

$$\bar{\bar{F}}(-k_z) \cdot \bar{\bar{Y}}_n(-k_z) \cdot \bar{\bar{T}}_{n,nm}(-k_z) = -(-1)^m \bar{\bar{F}}(k_z) \cdot \bar{\bar{Y}}_n(k_z) \cdot \bar{\bar{T}}_{n,nm}(k_z). \quad (61)$$

Hence (59) can be written as

$$L \approx -(-i)^m \frac{8}{\pi} \frac{ah}{\omega_{nm}\mu_0} |E_{nm}|^2 \mathbf{S}_{\phi nm}^t \cdot \tau_{nm} \quad (62)$$

where

$$\mathbf{S}_{\phi nm}^t = \int_0^{\infty} dk_z \sin\left(\frac{m\pi}{2} - k_z d_0\right) \mathbf{R}_{\phi n}^t(k_z) \cdot \bar{\bar{F}}(k_z) \cdot \bar{\bar{Y}}_n(k_z) \cdot \bar{\bar{T}}_{n,nm}(k_z). \quad (63)$$

Finally, we get the perturbational expression for the reso-

nance frequency of the wraparound cavity as

$$\omega_f \approx \omega_{nm} \left[1 - (-i)^{m+n} \frac{1}{2} \left(\frac{2}{\pi} \right)^2 \frac{1}{(1+\delta_{m0})} \frac{1}{d_0} \frac{1}{k_{nm}^2} S_{\phi nm}^t \cdot \tau_{nm} \right]. \quad (64)$$

For the cylindrical-rectangular patch, using (50) we obtain

$$L \approx (-i)^{m+n} \left(\frac{4}{\pi} \right)^2 \frac{ah}{\omega_{nm} \mu_0} |E_{nm}|^2 V_{nm}^t \cdot \tau_{nm} \quad (65)$$

where

$$\begin{aligned} V_{nm} &= U_{\phi nm} + \frac{1}{a} U_{znm} \quad (66) \\ U_{\phi nm}^t &= \sum_{r=1}^{\infty} r \frac{\sin \left(\frac{n\pi}{2} - r\phi_0 \right)}{r^2 - \left(\frac{n\pi}{2\phi_0} \right)^2} \\ &\cdot \int_0^{\infty} dk_z \sin \left(\frac{m\pi}{2} - k_z d_0 \right) \mathbf{R}_{\phi r}^t(k_z) \\ &\cdot \bar{\mathbf{F}}(k_z) \cdot \bar{\mathbf{Y}}_r(k_z) \cdot \bar{\mathbf{T}}_{r,nm}(k_z) \\ U_{znm}^t &= \sum_{r=0}^{\infty} \frac{1}{(1+\delta_{r0})} \sin \left(\frac{n\pi}{2} - r\phi_0 \right) \\ &\cdot \int_0^{\infty} dk_z k_z \frac{\sin \left(\frac{m\pi}{2} - k_z d_0 \right)}{k_z^2 - \left(\frac{m\pi}{2d_0} \right)^2} \mathbf{R}_{zr}^t(k_z) \cdot \bar{\mathbf{Y}}_r(k_z) \cdot \bar{\mathbf{T}}_{r,nm}(k_z) \quad (67) \end{aligned}$$

and

$$\begin{aligned} \mathbf{R}_{zr}(k_z) &= \frac{i\pi}{2h} \int_a^b d_{\rho} \mathbf{R}_{zr}(\rho, k_z) \\ &\approx \begin{bmatrix} 0 \\ 1 \end{bmatrix} \frac{1}{k_{1\rho} a} \frac{1}{J_r(k_{1\rho} a)} \frac{1}{J'_r(k_{1\rho} a)} \quad (68) \end{aligned}$$

where we have employed the symmetrical properties of the integrands.

Finally, we get the perturbational expression for the resonance frequency of the cylindrical-rectangular cavity as

$$\begin{aligned} \omega_f &\approx \omega_{nm} \left[1 + 2(-i)^{m+n} \left(\frac{2}{\pi} \right)^2 \right. \\ &\quad \left. \cdot \frac{1}{(1+\delta_{m0})} \frac{1}{(1+\delta_{n0})} \frac{1}{\phi_0 d_0} \frac{1}{k_{nm}^2} V_{nm}^t \cdot \tau_{nm} \right]. \quad (69) \end{aligned}$$

Thus (64) and (69) provide a perturbational approximation of the resonance frequencies of the wraparound and the cylindrical-rectangular cavity, respectively.

V. NUMERICAL RESULTS

The resonance in wraparound and cylindrical-rectangular microstrip patch resonators is presented using two different approaches: Galerkin's method (GM) and the perturbation approach (PA).

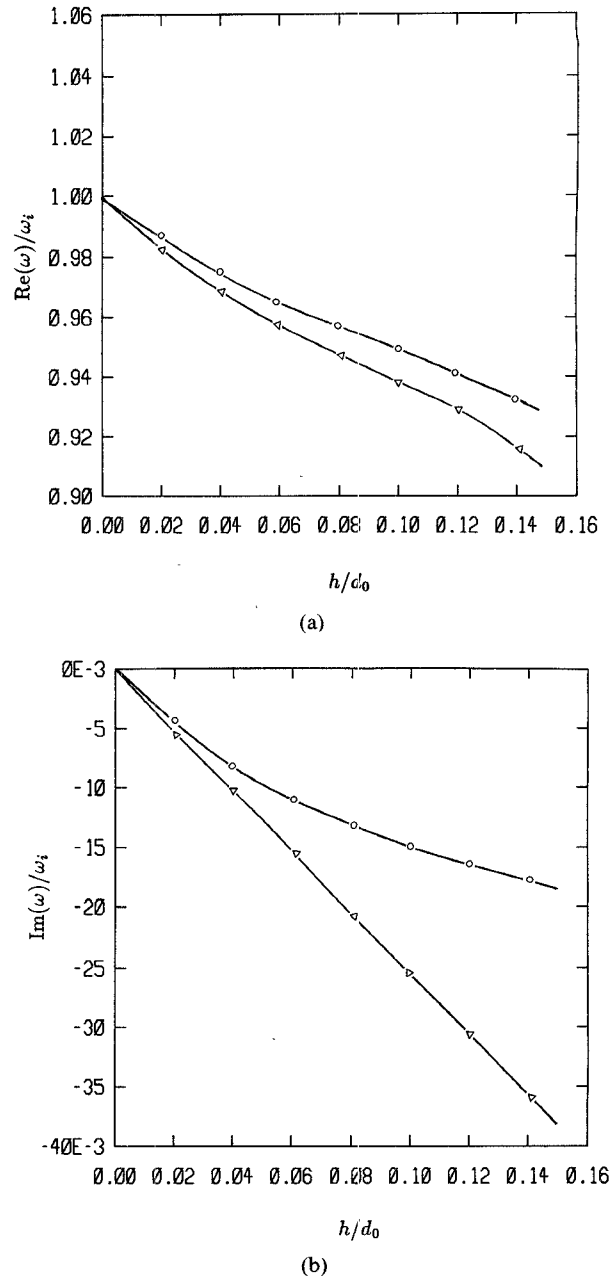


Fig. 2. (a) Real part of the normalized resonant frequency of a wraparound microstrip patch: $\epsilon_1 = 2.3\epsilon_0$, $a = 20$ cm, $d_0 = 4$ cm, TE_{01} mode, —○— (GM), —△— (PA). (b) Imaginary part of the normalized resonant frequency of a wraparound microstrip patch: $\epsilon_1 = 2.3\epsilon_0$, $a = 20$ cm, $d_0 = 4$ cm, TE_{01} mode, —○— (GM), —△— (PA).

In applying Galerkin's method and evaluating the matrix elements $|\bar{Q}_{pq,nm}|$ given by (39) or (40), the path of integration in the complex k_z plane has to be defined. Since the resonance frequencies are complex due to the radiation loss, the branch point and pole singularities can move below the real axis of the complex k_z plane. Therefore, the integration path is deformed below the real axis so that it does not cross the migration path of the singularities [9], [13].

Numerical results presented in this paper show the real and imaginary parts of the resonance frequencies for the

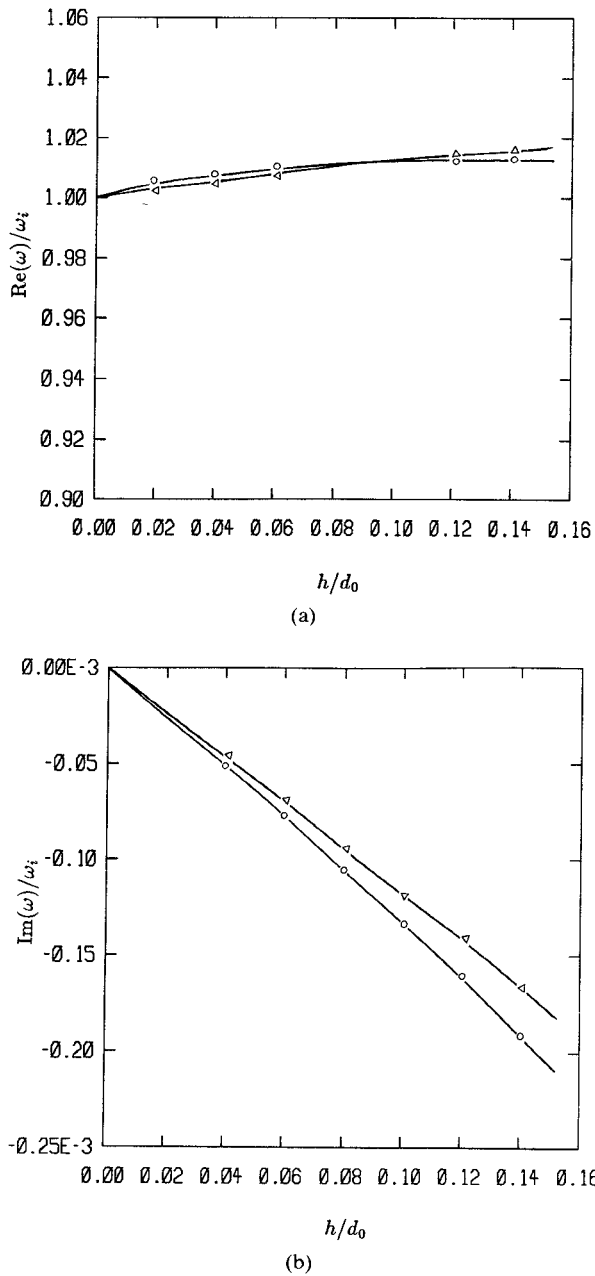


Fig. 3. (a) Real part of the normalized resonant frequency of a wraparound microstrip patch: $\epsilon_1 = 2.3\epsilon_0$, $a = 20$ cm, $d_0 = 4$ cm, HE_{10} mode, —○— (GM), —△— (PA). (b) Imaginary part of the normalized resonant frequency of a wraparound microstrip patch: $\epsilon_1 = 2.3\epsilon_0$, $a = 20$ cm, $d_0 = 4$ cm, HE_{10} mode, —○— (GM), —△— (PA).

wraparound and cylindrical-rectangular microstrip patches. The quality factor and the fractional bandwidth can be directly computed using the following expressions [14]:

$$Q = \frac{\omega'}{2\omega''} \quad \text{B.W.} = \frac{1}{Q}$$

where ω' and ω'' are the real part and the imaginary part of the resonance frequency, respectively.

In Fig. 2(a) and (b), the real and imaginary parts of the normalized resonance frequency of the TE_{01} mode for the wraparound resonator are displayed as a function of h/d_0 . The normalization is with respect to ω_i of the magnetic-wall

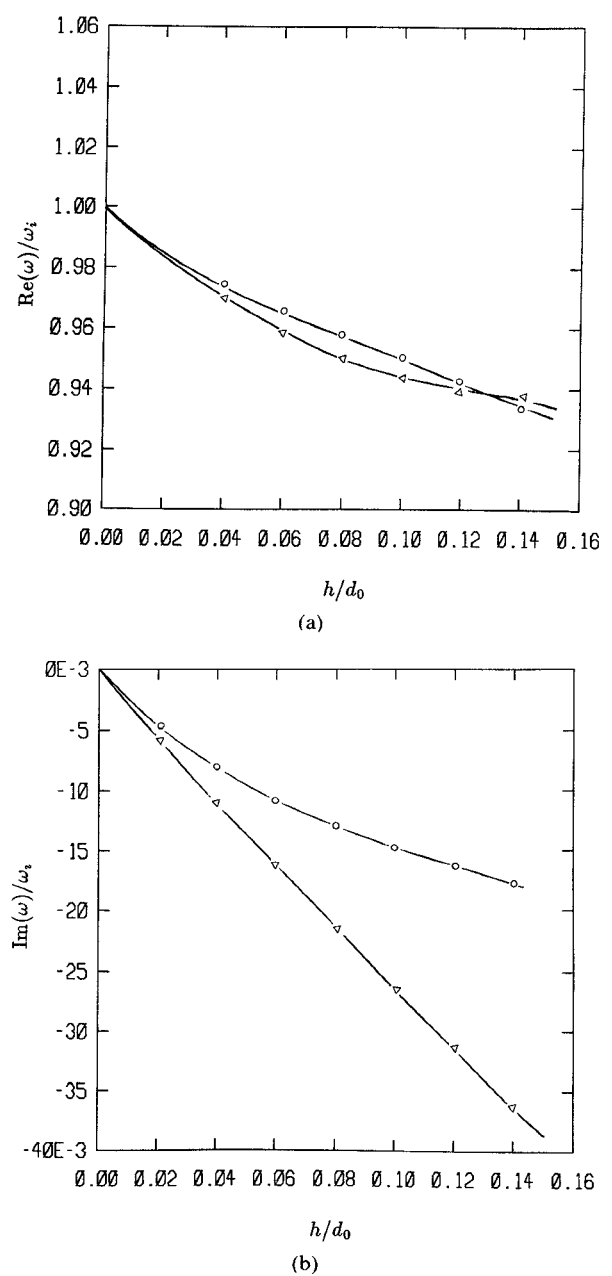
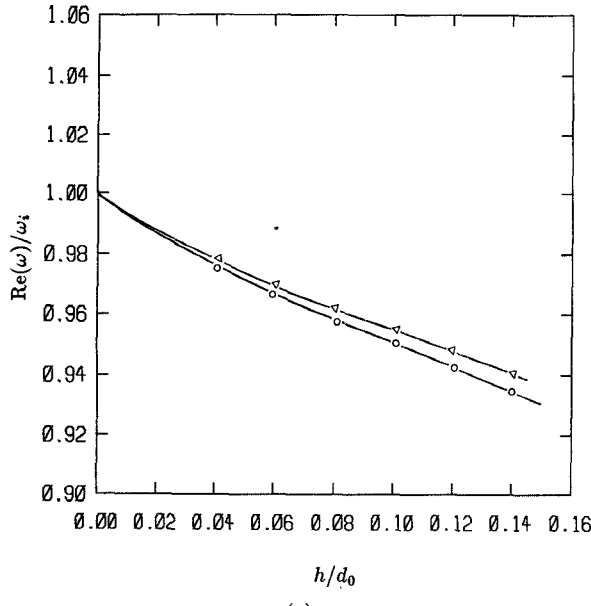


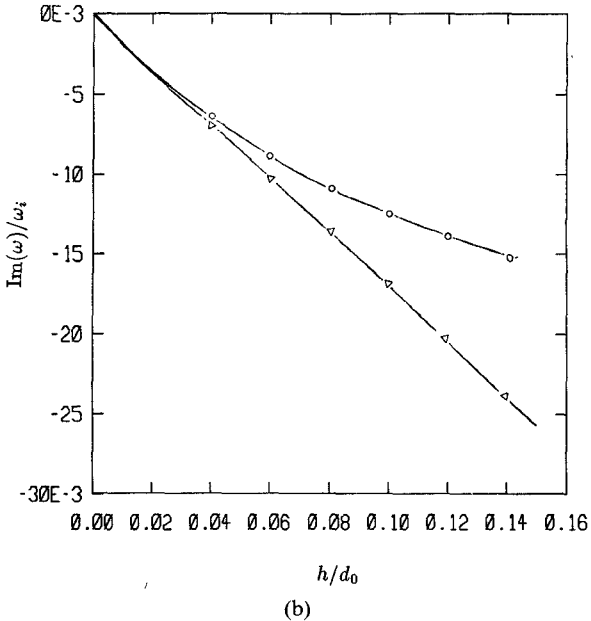
Fig. 4. (a) Real part of the normalized resonant frequency of a wraparound microstrip patch: $\epsilon_1 = 2.3\epsilon_0$, $a = 20$ cm, $d_0 = 4$ cm, HE_{11} mode, —○— (GM), —△— (PA). (b) Imaginary part of the normalized resonant frequency of a wraparound microstrip patch: $\epsilon_1 = 2.3\epsilon_0$, $a = 20$ cm, $d_0 = 4$ cm, HE_{11} mode, —○— (GM), —△— (PA).

cavity. In the calculation using Galerkin's method, the basis functions with $n = -1, 0, 1$ and $m = 0, 1, 2$ are employed. Basis functions without edge condition have been used, and the computed results for the resonance frequency are found to differ by at most 0.3 percent. The results using the perturbation approach and Galerkin's method are shown to be asymptotic to each other for a thin dielectric layer.

Fig. 3(a) and (b) shows the real and imaginary parts of the complex resonance frequencies of the HE_{10} mode for the wraparound resonator for a substrate with a dielectric constant of 2.3. Fig. 4(a) and (b) shows the real and imaginary parts of the complex resonance frequencies of the HE_{11} mode for the wraparound resonator for a substrate with a dielectric constant of 2.3. The results are shown to be asymptotic to each other for a thin dielectric layer.



(a)



(b)

Fig. 5. (a) Real part of the normalized resonant frequency of a cylindrical-rectangular microstrip patch: $\epsilon_1 = 2.3\epsilon_0$, $a = 20$ cm, $d_0 = 4$ cm, $\phi_0 = 24^\circ$, HE_{01} mode, —○— (GM), —△— (PA). (b) Imaginary part of the normalized resonant frequency of a cylindrical-rectangular microstrip patch: $\epsilon_1 = 2.3\epsilon_0$, $a = 20$ cm, $d_0 = 4$ cm, $\phi_0 = 24^\circ$, HE_{01} mode, —○— (GM), —△— (PA).

the HE_{11} mode for the wraparound resonator for a substrate with a dielectric constant of 2.3.

For the cylindrical-rectangular resonators, basis functions with $m = 0, 1, 2$ and $n = 0, 1, 2$ are employed in Galerkin's method. Eleven terms for the summation over r in (40), (66), and (67) are found to be sufficient to obtain convergent results.

Fig. 5(a) and (b) shows the resonance frequencies of the HE_{01} mode of the cylindrical rectangular microstrip resonator using a dielectric constant of 2.3. It is also found that the results using basis functions without edge singularity differ from that with edge singularity by at most 0.5 percent.

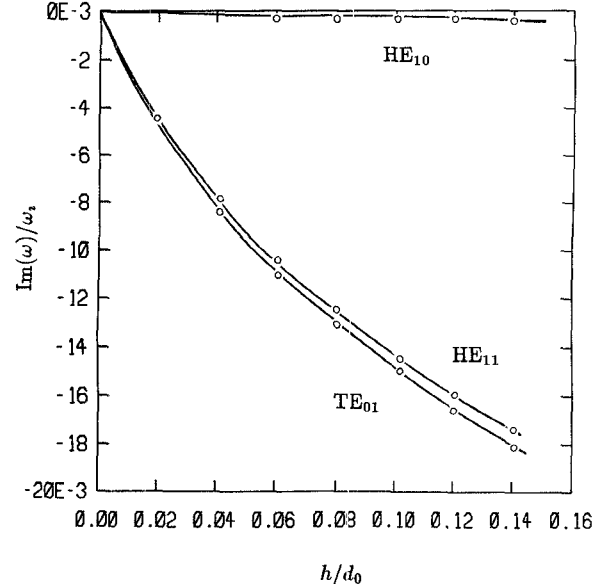


Fig. 6. Imaginary part of the normalized resonant frequency of a wraparound microstrip patch: $\epsilon_1 = 2.3\epsilon_0$, $a = 20$ cm, $d_0 = 4$ cm, —○— (GM).

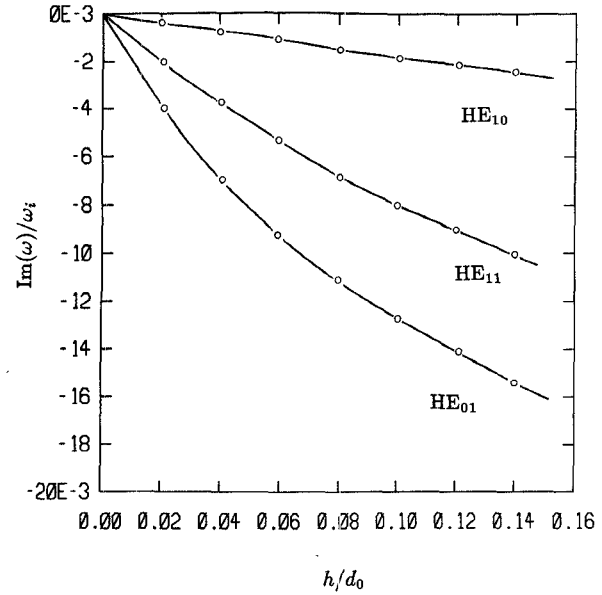


Fig. 7. Imaginary part of the normalized resonant frequency of a cylindrical-rectangular microstrip patch: $\epsilon_1 = 2.3 > \epsilon_0$, $a = 20$ cm, $d_0 = 4$ cm, $\phi_0 = 24^\circ$, —○— (GM).

In Fig. 6, a comparison of the imaginary parts of the resonance frequency for three different modes of the wraparound patch is displayed. Results indicate that the TE_{01} mode and the HE_{11} mode are the efficient radiating modes, having about the same radiating loss, and that the HE_{10} mode is more appropriate for resonator applications.

In Fig. 7, a comparison of the imaginary parts of the resonance frequency for three different modes of the cylindrical-rectangular patch is displayed. Results indicate that the HE_{01} mode is the most efficient radiating mode among these three modes, and that the HE_{10} mode is more appropriate for resonator applications. The radiation loss of the HE_{10} mode of the cylindrical-rectangular patch is

larger than that of the HE_{10} mode of the wraparound patch.

VI. CONCLUSIONS

A rigorous analysis of the resonance frequency problem of both the cylindrical-rectangular and the wraparound microstrip structure is presented using two different methods: an integral equation formulation and a perturbation approach. Using Galerkin's method in solving the integral equations, the complex resonance frequencies are studied with sinusoidal basis functions. The edge singularity of the patch current is shown to have no significant effect on the accuracy of the results. Furthermore, it is shown that the HE_{10} modes of the cylindrical-rectangular and wraparound patches are more appropriate for resonator applications. The HE_{01} and TE_{01} modes of the cylindrical-rectangular and wraparound patches, respectively, are efficient radiating modes.

REFERENCES

- [1] R. E. Munson, "Conformal microstrip antennas and microstrip phased array," *IEEE Trans. Antennas Propagat.*, vol. AP-22, pp. 74-78, Jan. 1974.
- [2] I. Wolff and N. Knoppik, "Rectangular and circular microstrip disk capacitors and resonators," *IEEE Trans. Microwave Theory Tech.*, vol. MTT-22, pp. 857-864, 1974.
- [3] T. Itoh, "Analysis of microstrip resonators," *IEEE Trans. Microwave Theory Tech.*, vol. MTT-22, pp. 946-952, 1974.
- [4] W. C. Chew and J. A. Kong, "Resonance of the axial symmetric modes in microstrip disk resonators," *J. Math. Phys.*, vol. 21, no. 3, pp. 582-591, 1980.
- [5] W. C. Chew and J. A. Kong, "Resonance of non-axial symmetric modes in circular microstrip resonators," *J. Math. Phys.*, vol. 21, no. 10, pp. 2590-2598, Oct. 1980.
- [6] S. M. Ali, W. C. Chew, and J. A. Kong, "Vector Hankel transform analysis of annular-ring microstrip antenna," *IEEE Trans. Antennas Propagat.*, vol. AP-30, pp. 637-644, July 1982.
- [7] S. M. Ali, T. M. Habashy, and J. A. Kong, "Resonance in two coupled circular microstrip disk resonators," *J. Appl. Phys.*, vol. 53, no. 9, pp. 6418-6429, Sept. 1982.
- [8] T. M. Habashy and J. A. Kong, "Coupling between two circular microstrip disk resonators," *Electromagnetics*, vol. 3, pp. 347-370, 1983.
- [9] W. C. Chew and Q. Liu, "Resonance frequency of rectangular microstrip path," *IEEE Trans. Antennas Propagat.*, vol. 36, pp. 1045-1057, Aug. 1988.
- [10] C. M. Krowne, "Cylindrical-rectangular microstrip antenna," *IEEE Trans. Antennas Propagat.*, vol. AP-31, Jan. 1983.
- [11] A. Naser, "Microstrip antennas on cylindrical structures," M.S. thesis, Military Technical College, Cairo, Egypt, 1987.
- [12] J. A. Kong, *Theory of Electromagnetic Waves*. New York: Wiley-Interscience, 1975.
- [13] N. Fache and D. De Zutter, "Rigorous full-wave space-domain solution for dispersive microstrip lines," *IEEE Trans. Microwave Theory Tech.*, vol. 36, pp. 731-737, Apr. 1988.
- [14] R. E. Collin, *Foundations for Microwave Engineering*. New York: McGraw-Hill, 1966.

From 1981 to 1982 he was a visiting scientist at the Research Laboratory of Electronics, MIT, Cambridge, MA. Since 1987, he has again been a visiting scientist there. His current research interests deal with microwave integrated circuits and microstrip antenna applications.

★

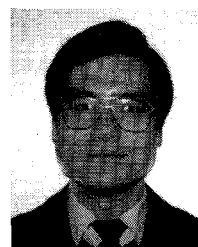


Tarek M. Habashy (S'79-M'83) was born in Cairo, Egypt. He received the B.Sc. degree from Cairo University, Egypt, and the M.Sc. and Ph.D. degrees from the Massachusetts Institute of Technology, Cambridge, MA, in 1976, 1980, and 1983, respectively, all in electrical engineering. During the academic year 1982-1983, he was a Postdoctoral Research Associate in the Department of Electrical Engineering and Computer Science at MIT.

Since September 1983, he has been with Schlumberger-Doll Research, Ridgefield, CT, as a member of the professional staff and is now the program leader of the Applied Electromagnetics Program, conducting research on inverse scattering and electromagnetic well-logging techniques.

Dr. Habashy currently serves as a member of the editorial board of the *Journal of Electromagnetic Waves and Applications (JEWAA)*. He is a member of AGU and Commission B of URSI.

★

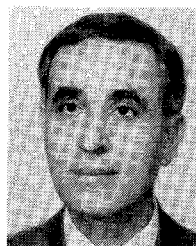


Jean-Fu Kiang was born in Taipei, Taiwan, R.O.C., on February 2, 1957. He received the B.S. and M.S. degrees in electrical engineering from National Taiwan University in 1979 and 1981, respectively. In 1983, he became a research and teaching assistant in the Department of Electrical Engineering and Computer Science at M.I.T., where he obtained the M.S. and Ph.D. degrees in 1985 and March 1989, respectively.

Since then, he has been working at IBM Research, Yorktown Heights, N.Y. His research interests are electromagnetic theory and applications and numerical analysis.

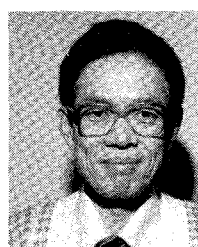
Dr. Kiang is a member of Sigma Xi.

★



Sami M. Ali (M'79-SM'86) was born in Egypt on December 7, 1938. He received the B.S. degree from the Military Technical College, Cairo, Egypt, in 1965, and the Ph.D. degree from the Technical University of Prague, Prague, Czechoslovakia, in 1975, both in electrical engineering.

He joined the Electrical Engineering Department, Military Technical College, Cairo, in 1975. In 1985, he became a Professor and head of the Basic Electrical Engineering Department there.



Jin Au Kong (S'65-M'69-SM'74-F'85) is Professor of Electrical Engineering, Chairman of Area IV on Energy and Electromagnetic Systems in the Department of Electrical Engineering and Computer Science, and Director of the Center for Electromagnetic Theory and Applications (CETA) in the Research Laboratory of Electronics at the Massachusetts Institute of Technology, Cambridge, MA.

During the years 1977-1980 he served the United Nations as a High-Level Consultant to the Under-Secretary-General on science and technology, and as an Inter-

gional Advisor on remote sensing technology for the Department of Technical Cooperation for Development. He was a Consultant to the New York Port of Authority (1971), the Army Engineering Topographical Laboratory (1979), the Hughes Aircraft Company (1981), the Lockheed Missiles and Space Company (1984-1986), the Raytheon Company (1979-1989), the Schlumberger-Doll Research Center (1985-1989), and the MIT Lincoln Laboratory (1979-1989). He also served as an External Examiner for the Electronics Department of the Chinese University of Hong Kong (1981-1983) and the University of Malaysia (1984), a Distinguished Lecturer of the IEEE Antennas and Propagation Society (1982-1984), an external reviewer for the Naval Research Laboratory (1989), and a member of the Advisory Council for the Electrical Engineering Department at the University of Pennsylvania (1987-1989).

His research interest is in the area of electromagnetic wave theory and

applications. He has published five books and over 200 refereed journal articles and conference papers and has supervised over 90 theses. He has been reviewer for numerous journals, government organizations, and book companies. He is the Editor for the Wiley Series in Remote Sensing, the Editor-in-Chief of the *Journal of Electromagnetic Waves and Applications (JEW)*, and the Chief Editor for the Elsevier book series on Progress in Electromagnetics Research (PIER).

Dr. Kong is a member of Commissions B, C, E, F, and H of the International Union of Radio Science (RSI), Phi Tau Phi, Tau Beta Pi, and Sigma Xi. He received the excellence in teaching award from the graduate student council at MIT in 1985. He is listed in *American Men of Science* (1969), *Notable Americans of the Bicentennial Era* (1976), *International Who's Who in Education* (1980), *Who's Who in the World* (1985), and *Who's Who in America* (1986).